



Molecular self-assembly and passivation of GaAs (001) with alkanethiol monolayers: A view towards bio-functionalization

J.J. Dubowski^{a,*}, O. Voznyy^b, G.M. Marshall^{a,c}

^a Department of Electrical and Computer Engineering, Université de Sherbrooke, Sherbrooke, Québec, J1K 2R1, Canada

^b Institute for Microstructural Sciences, National Research Council of Canada, Ottawa, Ontario, K1A 0R6, Canada

^c Institute for Chemical Process and Environmental Technology, National Research Council of Canada, Ottawa, Ontario, K1A 0R6, Canada

ARTICLE INFO

Article history:

Available online 2 April 2010

Keywords:

Self-assembled monolayers
n-Alkanethiols
passivation of GaAs
Bio-chemical sensing architectures

ABSTRACT

Properties of as prepared or nanoengineered III–V semiconductor surfaces provide attractive means for photonic detection of different adsorbants from surrounding gaseous or liquid environments. To be practical, this approach requires that the surface is made selectively sensitive (functionalized) to targeted species. In addition, such surface has also to stay stable over extended period of time to make it available for rapid testing. Numerous reports demonstrate attractive properties of GaAs for sensing applications. One of the most fundamental issues relevant to these applications concerns the ability to functionalize chemically, or biologically, the surface of GaAs. The most studied method of GaAs surface functionalization is based on formation of self-assembled monolayers (SAMs) of various *n*-alkanethiols, HS-(CH₂)_{*n*}-T (T = CH₃, COOH, NH₂, etc.). In spite of multi-year research concerning this issue, it has only been recently that a comprehensive picture of SAMs formation on GaAs and an understanding of the natural limitation of the SAM–GaAs interface in some bio-chemical sensing architectures has begun to emerge.

© 2010 Published by Elsevier B.V.

1. Introduction

Sensing based on the analysis of surface phenomena is an attractive approach for the detection and identification of biomolecules and chemical species with the potential to advance molecular diagnostics and other biomedical applications [1–3]. For metal surfaces such as Au, the fundamental interface applied in numerous biosensing architectures is based on the formation of self-assembled monolayers (SAMs) of various thiol group (R–SH) molecules [4–6]. SAMs of thiols have also been investigated for biofunctionalization of the GaAs (001) surface [7–12]. The functioning of electrical and optical devices based on the SAM–GaAs interface depends heavily on the quality of such an interface defined by both its sensitivity and stability. In spite of multi-year research concerning this issue, it has only been recently that a comprehensive picture of SAMs formation on GaAs and an understanding of the natural limitation of the SAM–GaAs interface in biosensing architectures has begun to emerge. In our research focused on the development of III–V photonic biosensing devices, the understanding of the role the GaAs surface plays in providing conditions attractive for anchoring bio-receptors is of paramount importance. GaAs – arguably the most studied representative of III–V semiconductors, in addition to

being attractive as a transducer for chemical or biological sensing [13,14], is also technologically important for quantum microstructures, such as InAs quantum dots, that use it as the capping material. We have suggested that photoluminescence (PL) from InAs self-assembled QDs grown epitaxially on GaAs, and capped with GaAs, could be used to monitor biochemical reactions taking place on the surface of the GaAs cap [15,16]. Our approach differs from so-called colloidal QD (cQD) biosensing [17], because we used optical emission from epitaxial QD to monitor surface properties of the cap layer material, while the cQD approach employs PL emission to beacon their presence, or the presence of biomolecules that they interact with. The strong intensity PL signal is important in such a case because it allows one to study surface properties under weak excitation conditions, i.e., such that they would not perturb the process of immobilization of biomolecules on the surface. The advantage of epitaxial QD is that they do not exhibit the so called ‘blinking effect’ that is known to limit significantly practical applications of cQD for biosensing [18]. Recently, we have demonstrated that epitaxially grown GaAs that is confined between the wide bandgap AlGaAs material, could provide a strong PL signal useful in the study of formation dynamics of SAMs on GaAs [19]. The enhancement of the PL signal has been observed in that case *in situ* as a function of time required for the formation of a thiol–GaAs interface. The significance of this experiment is that it suggests that some surface phenomena of III–V semiconductors could be studied by optical means with properly nanoengineered microstructures buried below such surfaces. Microscopically, the mechanism of

* Corresponding author. Tel.: +1 819 821 8000; fax: +1 819 821 7937.

E-mail address: jan.j.dubowski@usherbrooke.ca (J.J. Dubowski).

URL: <http://www.dubowski.ca> (J.J. Dubowski).

enhanced PL is not well understood. It has been linked with the modification (reduction) of the surface density of states that are known to act as non-radiative recombination centers [20]. This could be due to the chemisorption of sulfur atoms on As and/or Ga sites [13]. However, it has been reported that physisorbed oxygen could also have the similar effect [21].

The purpose of this paper is to review the results of theoretical and experimental studies addressing mechanisms of the formation of *n*-alkanethiol SAMs on the surface of GaAs, and the stability and functionality of SAM–GaAs interfaces. The paper does not claim to be a thorough review of the effort addressing the physics and chemistry of the *n*-alkanethiol SAM–GaAs interfaces. Instead, our intention was to provide the background material to introduce the problem and point out important directions of future research.

2. First principle investigations

2.1. Bonding nature of thiols on GaAs surfaces at low coverage

Experimental techniques typically used for investigation of prototypical organic monolayers on metal surfaces often are not accessible for semiconductors (e.g., STM, due to lower conductivity of the substrate) or are less informative due to inherent complexities of the semiconductor surfaces (e.g., exhibiting more complex surface reconstructions and consisting of several different chemical species). In this situation, theoretical modeling becomes an invaluable complementary tool for investigation.

Several theoretical studies of the short-chain thiol adsorption on GaAs (001) at low coverage have been reported so far [22–26]. The first question required to be understood is the binding energy on different adsorption sites and the factors affecting it. Simplified models involving small molecular clusters or a small periodic unit cell were initially used to reduce the computation time. Early X-ray photoelectron spectroscopy (XPS) experiments suggested binding of thiols to As [11,27,28], thus most of the models were As-terminated and mimicked the dimerization of As typically observed on GaAs surfaces. All of the reports agreed on the preferred formation of a single covalent bond between thiolate sulfur and one of the arsenic species, with the bond energy ~ 2 eV. This bond is stronger than S–Au bond of thiolates on gold surfaces and has a more covalent and directional character [22] which may impose additional constraints on subsequent adsorption geometries and self-assembly of thiols.

Intuitively, one can expect different binding energies of thiolate depending on surface termination, i.e., depending on whether S–Ga or S–As bond is formed. Interestingly, S–Ga bond was found to be 2.8 eV for a single thiolate adsorbed on a clean surface, i.e., stronger than S–As bond, despite the absence of visible signs of the former in the XPS data. However, surface reconstruction was found to play an even more important role. Our density-functional theory (DFT) calculations with bigger surface unit cells corresponding to Ga-rich as well as As-rich conditions [22,23] revealed drastic changes of binding energy depending on surface conditions, such as surface reconstruction, presence of hydrogen on the surface, coverage of thiols and even their relative adsorption sites. Fig. 1 summarizes our findings.

Investigation of surface relaxation upon adsorption and shapes of the molecular orbitals [22,23] allowed us to explain the observed variations in thiolate–surface bond energies. It was found that the electron counting rule [29] responsible for peculiar surface reconstructions of the free semiconductor surfaces also plays a crucial role in defining whether or not thiol adsorption would be favorable. This simple empirical rule states that the most stable surface reconstruction does not possess partially filled dangling bonds (which would form mid-gap surface states and increase the total energy of the system). For GaAs this means that the dangling bonds of Ga

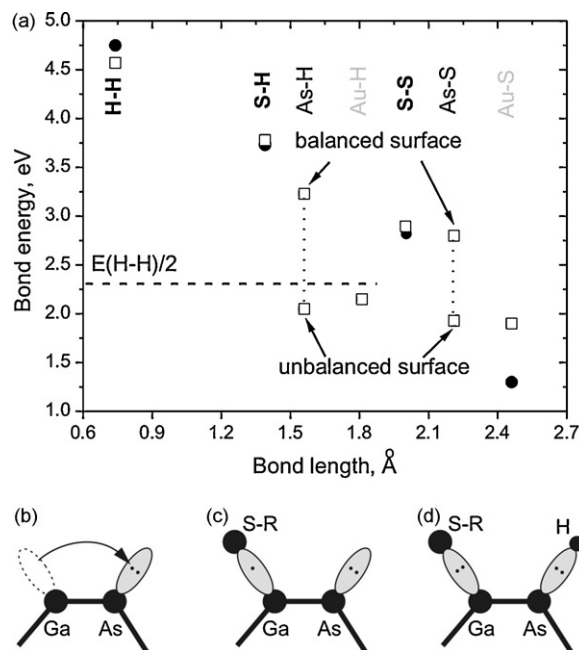


Fig. 1. (a) Energies of the bonds involved in thiol adsorption on GaAs (001) and Au (111) surfaces. Full circles, experimental data; open squares, our calculations. As–H and As–S values are presented for different surface conditions (see text for details). Theoretical values for Au–S are for br-fcc adsorption site. (b–d) Schematic representation of electron counting rule: (b) clean surface, (c) breaking the balance upon thiolate adsorption, and (d) restored balance when two species are adsorbed.

should be empty while those of the more electronegative As should contain 2 electrons each. We term such a surface ‘balanced’ in Fig. 1. Similarly to the most stable surface reconstruction, the most stable thiol adsorption site (and thus the strongest thiolate–surface bond) would be such that results in a balanced surface.

Due to the nature of thiolate adsorption via formation of a single covalent bond to the surface, thiolate brings only one electron to the surface. Thus, adsorption on a clean surface prepared in vacuum inevitably destroys the existing electronic balance, resulting in a weak thiolate–surface bond (Fig. 1c). The electronic balance can be however preserved if two species are adsorbed, e.g., on Ga and As sites, respectively (Fig. 1d).

2.2. Kinetics of adsorption and decomposition reactions of thiols on GaAs (001)

The sensitivity of the bond energy to adsorption site and to combination of the already occupied sites significantly affects the kinetics of the adsorption and desorption reactions, making the order of particular adsorption/desorption events as important as the energetics itself. Thus, it becomes crucial how the thiol is getting adsorbed in the first place.

Fig. 2 summarizes possible thiol reaction pathways on an As-rich (2×1) surface reconstruction (with one As–dimer per unit cell). Our simulations revealed that the presence of the physisorbed precursor is essential for the cleavage of the S–H bond [23]. Participation of the surface in this process produces a reduction in the energetic barrier from 3.75 eV (Fig. 2a) to only ~ 0.5 eV (Fig. 2c) and results in adsorption of both thiolate and hydrogen on nearby surface atoms. It was also found that on surfaces exposing both As and Ga atoms, adsorption of S on Ga is preferred resulting from a weak non-dissociative chemisorption state formed by the overlap of a sulfur lone pair orbital with an empty Ga dangling bond.

The energy required to cleave the S–As bond and to desorb thiolate (Fig. 2d) has a value of 2.1 eV, which based on the Readhead formula [30] corresponds to thermal energies ~ 700 K. However,

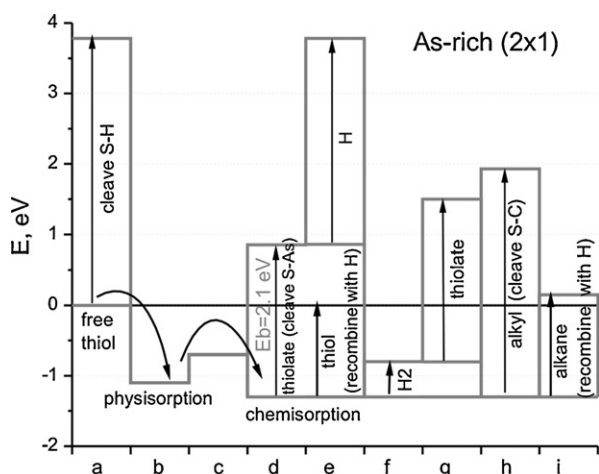


Fig. 2. Adsorption-desorption pathways and energetics of thiol on As-rich (2×1) surface reconstruction.

the presence of hydrogen adsorbed nearby makes the recombinative desorption process possible. This process (Fig. 2e) requires only 1.25 eV, i.e., slightly higher than room temperature, in line with experimental observations [31–33]. Adsorbed hydrogen can also recombine with another hydrogen already present on the surface, desorbing as a hydrogen molecule (Fig. 2f). Similar to the cleavage of S–As bond, cleavage of S–C bond is in principle possible but requires quite high energy of 3.2 eV (Fig. 2h). However, recombination of the alkyl part of the thiol with surface hydrogen and desorption as alkane, leaving sulfur on the surface, requires a much smaller energy of only 1.35 eV (Fig. 2i).

The exact surface reconstruction will significantly affect the relative energetics of the above reactions and may result in significantly different species remaining on the surface. It should be noted that As-rich (2×1) surface is initially electronically unbalanced and is expected to be similar to a disordered As-rich surface obtained after wet etching. Detailed theoretical analysis of the kinetic activation barriers and energetics of the above reactions was also performed for the balanced Ga-rich [23] and As-rich [25] surfaces. The results obtained are in good agreement with available temperature programmable desorption (TPD) data for thiols deposited in a vacuum [32–34], exhibiting desorption of molecular hydrogen, intact thiol, and alkane, along with the absence of thiolate desorption peaks in spectra. The most prominent difference from the results presented here is the much higher energy required for desorption of hydrogen from the surface. A facile desorption of hydrogen is also characteristic for thiol adsorption on Au (111) surface. Recently, it was confirmed experimentally that vacuum deposition from disulfides rather than from thiols significantly improves the stability of the resulting adsorbates due to elimination of hydrogen deposition and thus elimination of the recombinative desorption pathway [34].

2.3. SAMs commensurate with the GaAs (001) surface

Unpredictable initial reconstruction and adsorption sites, and constantly varying energetics of each single adsorption reaction make it practically impossible to model theoretically the outcome of thiol deposition on GaAs from liquid phase. Nevertheless, experimental infrared (IR) spectroscopy data show a high degree of crystallinity of alkanethiol SAMs on GaAs (001) [11,35]. Fitting of simulated IR peak intensities to experimental data also provides the tilt (deviation from surface normal) and twist (rotation about the chain axis) angles of the molecules in the SAM. Thus, the crystalline structure of thiols can be used as a valuable starting point for the

back-engineering of the thiol–GaAs interface structure. However, initial attempts to resolve the structure of thiol SAMs on GaAs using this approach were unsuccessful as it was found that the two crystalline structures are incommensurate if GaAs surface is assumed to be flat [35].

We approached the problem by asking the following question: how should the interface between a SAM and GaAs (001) look to accommodate the most densely packed structure of thiols? Our calculations have indicated the need to form interfaces comprising the trench–ridge–trench 3-dimensional (3D) surface reconstruction shown in Fig. 3 [36]. Obtained idealized structure possessed the macroscopical properties of the interface observed experimentally [35], and are similar to the typical As-rich reconstruction of the ideal surfaces prepared in a vacuum [37]. Hence, we have suggested that the thiol–thiol interactions are strong enough to enforce the required interface structure rather than leaving thiols to adapt to the surface reconstruction available after etching. We proposed that the method of searching for a 3D reconstructed surface could also be applied to Au surfaces accommodating densely packed thiols [38], which allowed us to interpret some of the experimental results [39]. This supports that our original prediction that the process of *n*-alkanethiol SAM formation on the GaAs surface could predict at least the most important features of the thiol–GaAs interface.

The introduction of atomic roughness of the surface overcomes the incommensurability of the SAM with the surface, owing to the exposure of more binding sites per unit area. At the same time, it increases the amount of surface sites uncovered by thiols, which may explain why only partial passivation by thiols on GaAs has been reported till today (including our results). An electronic balance of the surface, important for the stability of the SAM against desorption as well as for electronic passivation of the surface, can be preserved only if H remains adsorbed on the As sites uncovered by thiols. Whether or not such an ideal geometry is achieved in a highly dynamic process of SAM formation described above is not known. It should be noted that hydrogen cannot be adsorbed on Ga sites (see empty sites in Fig. 3) since it would be situated too close to the sulfur on the opposite side of the trench. Similarly, the distance between S atoms on different sides of the trench is only $\sim 4 \text{ \AA}$ (see Fig. 3a), facilitating desorption of disulfides. Analysis of the desorbing species in a TPD experiment could clarify more aspects of the proposed structure; however, the experimental TPD data is currently available only for thiols deposited in ultra-high vacuum. Depending on the results of such experimental verification, new strategies for improved stability of the SAMs could be developed, e.g., using disulfides instead of thiols [34], switching to a different surface orientation of GaAs [40,41] or even switching to another semiconductor material with a larger lattice constant, e.g., InAs [42].

3. Experimental

The parameters characteristic of a well-formed *n*-alkanethiol SAM on the GaAs (001) surface are manifold. In this section, we describe the results obtained from our studies using XPS, IR spectroscopy, Kelvin Probe and PL techniques. These results detail the molecular orientation, surface dipole layer potential (DLP) and IR optical constants of the SAMs. We also discuss the dynamics of SAM formation observed with *in situ* PL measurements.

3.1. X-ray photoelectron spectroscopy

Since the chemisorption of thiols accompanies the process of self-assembly, the observation of a S–GaAs chemical state is important to the verification of SAM formation. XPS measures chemical

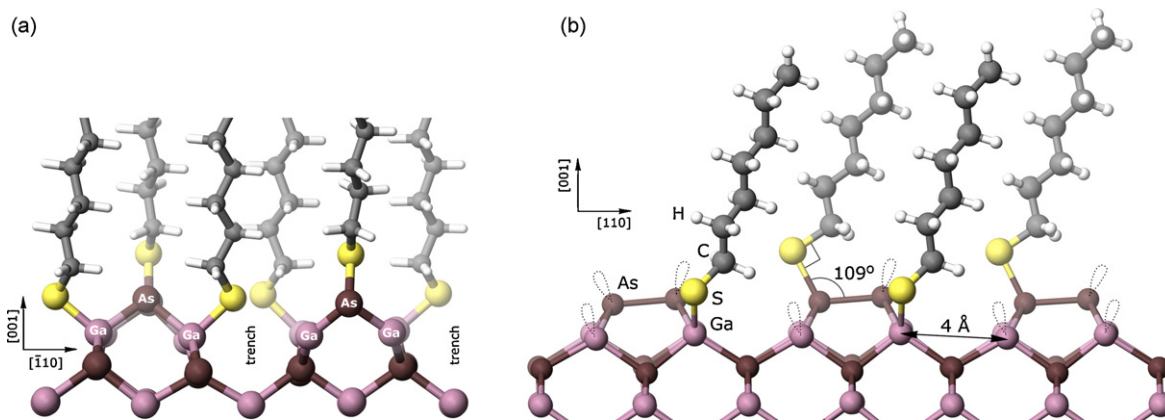


Fig. 3. (a) Front and (b) side views of the proposed structure for dense thiol SAMs on GaAs (001). The trenches along [110] direction expose the Ga-rich (111) plane. Dangling bonds, i.e., sites potentially available for thiol or hydrogen adsorption but remaining uncovered, are shown with dotted lines [36].

state changes as shifts in the binding energy of electrons. Binding energy shifts of about -1.5 eV have been reported [12,43,44], similar to that found on Au substrates [45,46]. The negative shift in binding energy characteristic of the S–GaAs bond is measured relative to its thiol (S–H) precursor and implies an increase in valence charge on the sulfur atom.

XPS can also be used to characterize the thickness of the overlayer associated with the SAM using angle-resolved (AR) XPS techniques. Most ARXPS methods reference the substrate on which the overlayer is formed [47,48], which can be complex owing to the account that has to be made of the GaAs stoichiometry at the interface. In the following result, ARXPS analysis was performed using only the atomic species within the SAM itself. The ratio of S 2p and C 1s emissions was tracked as a function of the photoelectron take-off angle, and an inelastic scattering model based on the ordered SAM was constructed in order to extract the average molecular chain axes tilt. The measurements indicated in Fig. 4 are for hexadecanethiol ($\text{HS}-(\text{CH}_2)_{15}-\text{CH}_3$) SAMs and the fitting computes to a value of $17 \pm 4^\circ$. This result agrees closely with literature reports ranging from 14° to 19° using near edge X-ray absorption fine structure [11], IR ellipsometry methods [49], grazing incidence X-ray diffraction (GIXRD) [35] and our own DFT modeling results [36].

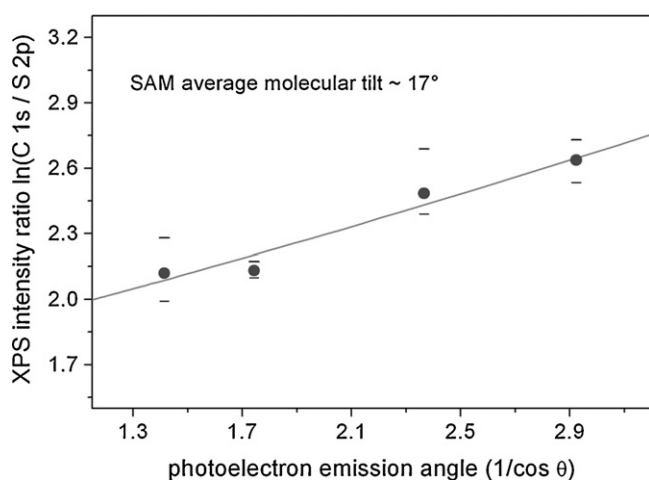


Fig. 4. ARXPS analysis of a hexadecanethiol ($\text{HS}-(\text{CH}_2)_{15}-\text{CH}_3$) SAM on the GaAs (001) surface. The C 1s/S 2p photoemission ratio was measured as a function of the normal emission angle and fitted with an attenuation model (line) to derive the average molecular tilt ($17 \pm 4^\circ$). Data are 3-spot averaged (circles) showing max/min values (bars).

With appropriate energy referencing, XPS can also be used to determine the work function of the surface. Since long-chain CH_3 terminated thiols can form a well-ordered two-dimensional (2D) array of molecules having outwardly directed dipole moments, as in Fig. 5, the work function change of the surface upon SAM formation is expected to be large. By electrically isolating the samples, they may be referred to the vacuum level (VL) such that decreases in binding energy relate to decreases in the work function. Assuming the surface Fermi level (FL) is pinned with respect to thiol treatment [20,27], the work function change may be interpreted in terms of the net change in electron affinity resulting from the addition of a 2D-DLP. Monitoring the As 3d photoemission, the binding energy shift observed upon formation of a hexadecanethiol SAM was about 300 meV, as illustrated in Fig. 6 [50]. We have also observed that the 2D-DLP is strongly chain length dependent, which, as discussed in the next section, has important implications in view of the observed IR absorption intensity.

3.2. Infrared spectroscopy and Kelvin Probe

Another means to establish the physical properties of SAMs is IR spectroscopy, which, for our material system, typically involves measuring the IR absorbance of the C–H stretching modes associated with the alkane chain axes. New and significant phenomena are associated with the SAMs, which are characterized using this sensitive technique. Exploiting the linearity observed in transmission mode data for SAMs with $n=11$ –17 methylene units, Beer–Lambert analysis was used to derive the spectrum of absorption coefficients for the SAM structure. As shown in Fig. 7, a comparison with values measured in liquid alkanethiol showed that the absorption coefficients are some 6 times higher than in the SAM phase [51]. Part of this is accounted for by molecular orientation and other intrinsic factors, however, at least a $3\times$ multiplier is due to extrinsic factors related to SAM formation as described in the following.

Using the Kelvin Probe technique, the 2D-DLP was evaluated by subtracting the work function associated with the ordered SAM

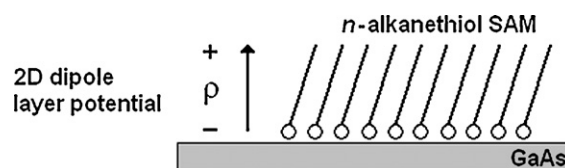


Fig. 5. Illustration of the 2D dipole layer potential formed by a SAM of n -alkanethiol on the GaAs (001) surface. Arrow indicates the direction of a sheet dipole moment [50].

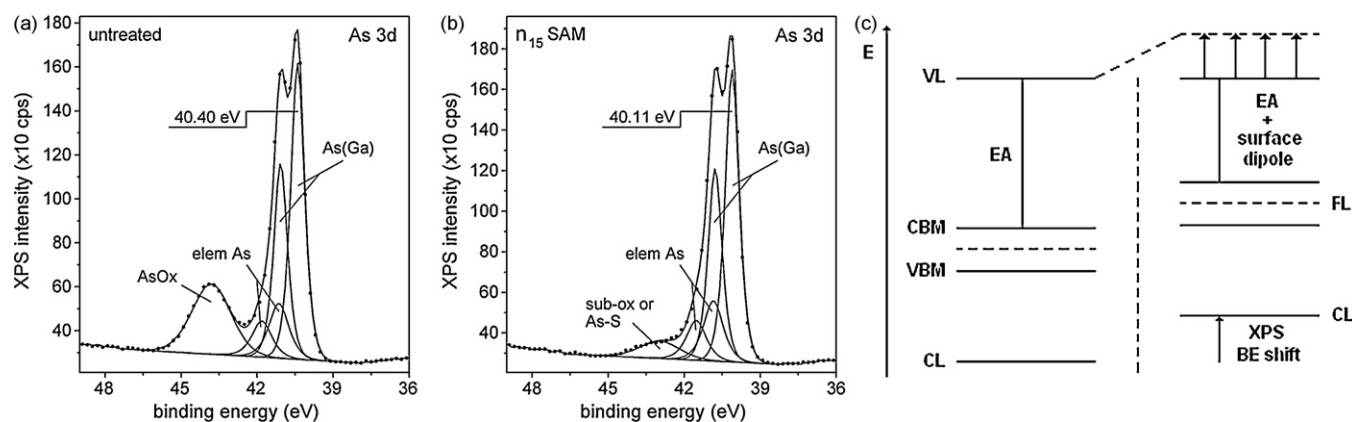


Fig. 6. XPS core level (CL) As 3d spectra from etched but untreated GaAs (001) (a) and from GaAs (001) prepared with hexadecanethiol SAM (b). Samples are electrically isolated such that spectra are referred to the vacuum level (VL) (c). The binding energy (BE) shift of ~ 300 meV indicates a change in potential corresponding to the surface dipole layer that reduces the electron affinity (EA). See Ref. [50] for component details.

phase from the work function measured after thermal disordering. Close agreement with the previously discussed XPS method was obtained. More importantly, we observed a direct proportionality between the 2D-DLP and the IR absorption intensity as a function of chain length, each scaling together at a rate well in excess ($3\times$) of the unitary increase expected. Fig. 8 demonstrates the strong linear correlation between the IR absorbance and the Kelvin Probe contact potential difference, from which the 2D-DLP was obtained [50]. We interpret this result to suggest that the 2D-DLP is associated with a uniformly polarized medium carrying a significant electrostatic field that enhances the electronic component of the molecular polarizability. This effect results in an increase of the IR oscillator strengths, i.e., in the resonant amplitude of the vibrational modes, which is observed as an enhancement of the IR activity.

One key aspect of both the IR and 2D-DLP results relates to the assumption that the SAMs are sufficiently well-ordered enough to support linear analysis. ARXPS studies report that the average molecular tilt of SAMs ranging from $n = 11$ to 17 is about 15° [48]. That the tilt values are consistent with n and concur with the values discussed above suggests that the SAMs meet with the assumed criteria. Furthermore, we have shown that a model decomposition of the IR spectra could be analyzed in terms of n -dependent components that scale linearly above a threshold value near $n = 10$ [51].

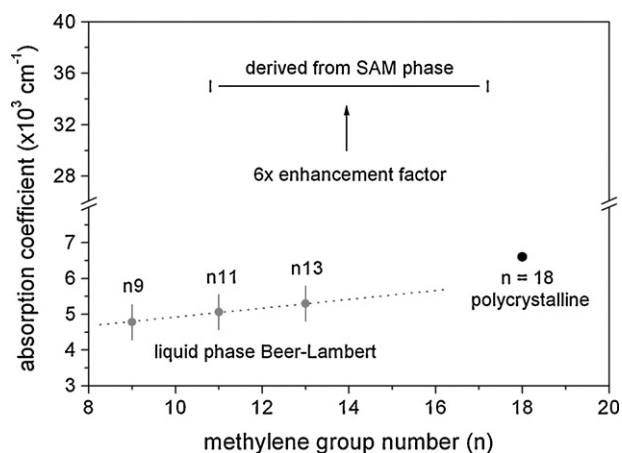


Fig. 7. SAM phase absorption coefficient relative to Beer–Lambert measurements in bulk material illustrating the $6\times$ enhancement factor. Polycrystalline $C_{19}H_{39}CO_2Na$ result borrowed from Parikh et al., J. Chem. Phys. 96 (1992) 927. Dotted line used for trend visualization only [51].

Perhaps of most interest in the discussion of SAM uniformity is that our results agree with those obtained from IR ellipsometry methods [49] used to derive the optical constants in the IR region. Employing suitable transformations, the absorption coefficients evaluated from our Beer–Lambert analysis [52] were used in conjunction with the structural parameters obtained from DFT calculations [36] in order to calculate the principle components of the refractive index tensor. Most notable among the DFT structural parameters is the uniaxial absorption asymmetry that it prescribes. Compared to IR ellipsometry data at $n = 15$, our Beer–Lambert analysis yielded identical optical constants, which are provided for reference in Fig. 9 [50]. Equivalence of the single point ellipsometry results [49] with ours obtained from linear analysis over several n -values enabled us to conclude that the SAMs were indeed highly uniform. Based on the n -consistency of the optical constants, the implication for the low-frequency dielectric permittivity is direct, which underscores the linearity observed in the 2D-DLP, where an effective capacitor model of the SAM is assumed.

3.3. Photoluminescence results

Our early PL experiments were focused on studying the effect the molecular terminal group (CH_3 , $COOH$, OH , etc.) has on SAM

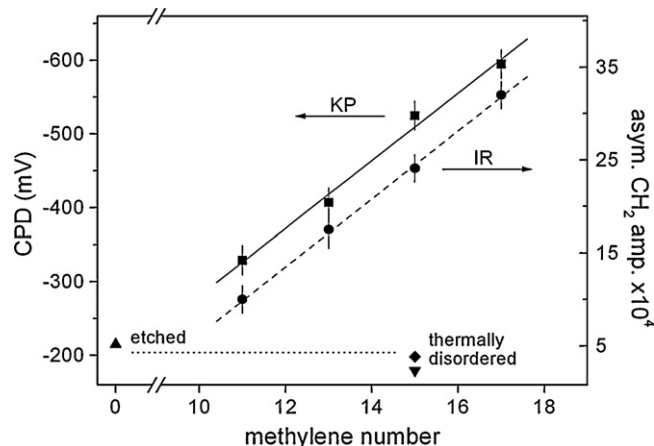


Fig. 8. Kelvin Probe (KP) contact potential difference (squares) and infrared (IR) asymmetric CH_2 stretching mode peak absorbance (circles) vs. chain length for $[HS-(CH_2)_n-CH_3]$ SAMs on semi-insulating GaAs (001). KP etched only GaAs (up triangle). KP (diamond) and IR (down triangle) thermally disordered n_{15} -SAM. Baseline work function (dotted line) used to reference the 2D dipole layer potential by subtraction [50].

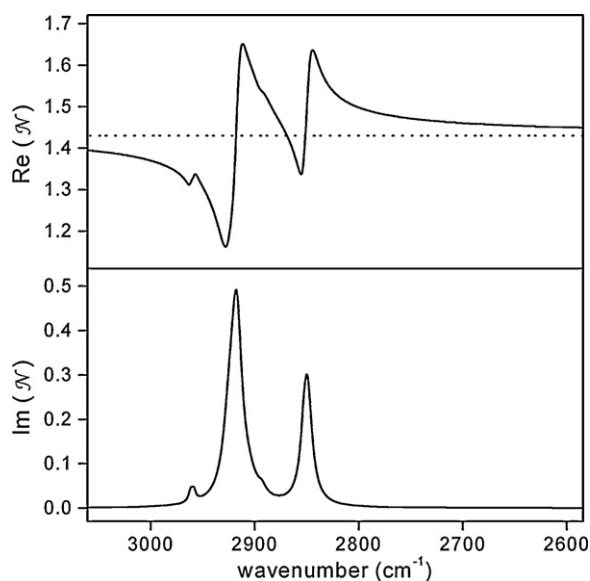


Fig. 9. Real (η) and imaginary (κ) parts of the refractive index (N) tensor in terms of the principal (diagonalized) components. Off-resonance isotropy (dotted line) with $\eta_{3,3} = 1.43$ is assumed. Uniaxial symmetry is applied such that $\eta_{1,1} = \eta_{2,2}$, $\kappa_{1,1} = \kappa_{2,2}$ and $\kappa_{3,3} = 0$ in the IR region defined [50].

formation [52] and the stability of the thiol–GaAs interface [41,53]. Varying the SAM terminal group from a hydrophilic to hydrophobic moiety resulted in an enhanced PL signal from the supporting GaAs (001) substrate. These results were corroborated by IR absorption spectroscopy of the methylene units, indicating that SAMs having hydrophobic terminal groups formed more vertically oriented monolayers. Consequently, SAMs with hydrophobic terminal groups provided better passivation of the GaAs surface relative to the hydrophilic SAMs.

While end-state and *ex situ* observations are useful to the study of SAM formation, *in situ* measurements provide controlled growth and analysis conditions yielding more precise results. Our group is the first to demonstrate the formation dynamics of alkanethiol SAMs on (001) GaAs using *in situ* PL measurements. The experimental system consists of a hyperspectral PL mapper (HI-PLM)

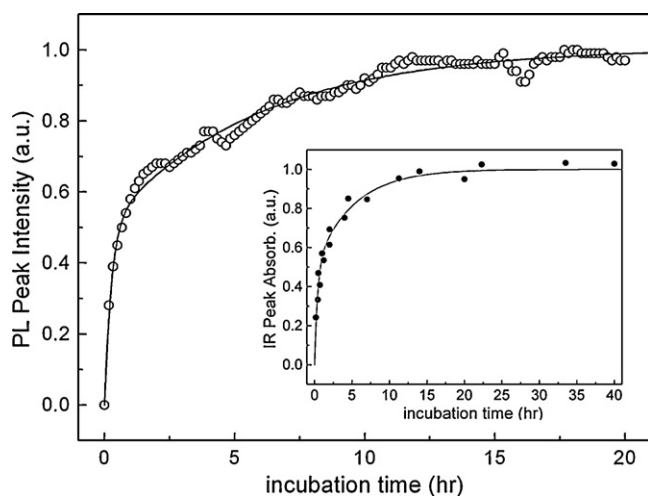


Fig. 10. Time evolution of the *in situ* PL peak intensity from an etched GaAs structure exposed to 2 mM of hexadecanethiol dissolved in degassed ethanol. PL is differential with respect to the PL from the structure similarly exposed to the ethanol solvent only. Inset: IR peak absorbance of the asymmetric C–H stretching mode of methylene in hexadecanethiol SAMs. Data are normalized to the respective saturation values of each curve [19].

with which the dynamics of SAM formation can be monitored in real-time [19]. Comparing the PL time series of GaAs in hexadecanethiol solution with GaAs similarly exposed to the ethanol solvent only, we observed a two-phased evolution of the associated PL enhancement. These PL measurements, as illustrated in Fig. 10, are corroborated by time-commensurate changes in the absorption intensity of the C–H stretching mode vibrations recorded using *ex situ* IR spectroscopy. The practical importance of these results is manifested in the sensitivity with which *in situ* PL monitoring can reflect surface processes, and underscores its potential for use in sensor applications. These findings are important to the model we are developing that will ultimately provide a quantitative understanding of sensor operation. We expect the mode of transduction will be electrostatic in nature, where the PL from strongly emitting III–V quantum semiconductor microstructures will be modulated by the fields associated with biomolecular charge.

4. Functionality of the SAM

The development of a biosensor platform relies critically on the functionality of the SAM–GaAs interface. Though more complex degrees of functionalization are required for practical applications, the demonstration of covalent bond attachment to the functional groups of a SAM is a relevant first step. To this end, we investigated biotin coupling to an amine-terminated (R–NH₂) SAM. Biotin is a protein-ligand typically employed in biochemical assays that forms a covalent bond with amine through its carboxylic acid group (R–COOH). In contrast with SAMs prepared with molecules of HS–(CH₂)₁₅–CH₃, we observed that the IR spectra of SAMs prepared with molecules of HS–(CH₂)₁₆–NH₂ displayed characteristics of a less-ordered monolayer, i.e., reduced amplitude and increased vibrational energies. It is possible that hydrogen bonding between the amine functional groups forms a partial bilayer [54], or the amine groups are charged (protonated) in the solution, which would resist the close-packing necessary for a higher degree of SAM order.

In terms of a surface passivating agent, a less ordered monolayer structure would provide a less effective barrier to reoxidation. Indeed, the avenue of approach to device design must ultimately account not only for functionality, but also must address the issue of interface stability in the environment of use (aqueous, physiological, etc.). An additional confounding factor to the establishment of a well-ordered SAM in the amine-terminated system may be the competition for surface bonding between the amine and thiol groups in solution. Both have nucleophilic character, but whereas thiol may present a charged and therefore more reactive species, the amine should form only a weak bond. Use of a neutral ethanol solution has ruled out significant amine–GaAs bonding in IR and XPS testing, though evidence of surface-bonded R–NH₂ species has been observed at other pH values.

Despite the reduced degree of molecular ordering and the possibility of inverted surface bonding, a strong S 2p signal indicative of chemisorption was observed as illustrated in Fig. 11 (left). Interestingly, a small S-oxide (S_xO_y) component can be seen that does not show up in methyl-terminated (CH₃) samples, but is expected if uncoupled thiol is present in the inverted or bilayer arrangement. Comparing the XPS N 1s signal before and after biotin coupling treatment, a significant increase in nitrogen concentration is observed in Fig. 11 (right). Our separate tests have ruled out direct biotin–GaAs coupling. Therefore, following that biotin carries two nitrogen atoms per molecule and that the additional nitrogen is due to covalently bonded biotin, a rough estimate of the degree of amide coupling to the functionalized surface of GaAs (001) is about 40%. This is a reasonable number given the estimated steric limit of 50% in the ideal SAM case. Examples of SAM-based

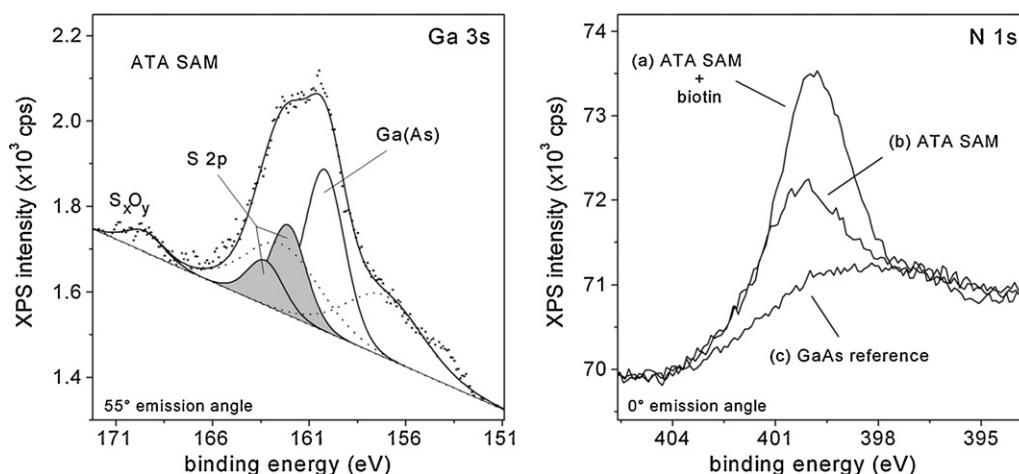


Fig. 11. Left: XPS Ga 3s spectral region of GaAs (001) prepared with amine-terminated (ATA) SAMs ($\text{HS}-(\text{CH}_2)_{11}-\text{NH}_2$). Component estimation: bulk phase Ga(As) (solid), Ga oxides and photoelectron losses (dotted), S 2p doublet at 162.1 eV (grey), and S_xO_y near 170 eV. Right: XPS N 1s spectra of the ATA SAM after (a) and before (b) biotin coupling. An attenuation factor was applied to the etched and untreated GaAs reference (c) to model the loss of intensity through the SAM. Spectra are vertically aligned for quantification purposes.

advanced architectures include specifically immobilized avidin on biotinylated thiols [55] and influenza A particles on biotinylated antibodies interfaced with neutravidin [56].

5. Conclusions

The ultimate success of the quantum semiconductor PL biosensor technology rests strongly on our understanding of the fundamental processes involved in the formation of the base interface between an organic layer and semiconductor, such as that of *n*-alkanethiol–GaAs. In addition to offering potential solutions for sensing applications, the *n*-alkanethiol SAM–GaAs interface has been of great interest for surface passivation [57] and, e.g., for molecular junction nanoelectronics [48] and nanolithography [58]. The full description of SAMs formation on GaAs is still missing, but several aspects of this process have become more clear as a result of the research reported in this review and referenced literature. The incommensurability of the *n*-alkanethiol SAM with the GaAs (001) surface results in the natural presence of surface sites left uncovered by thiols. Thus, new strategies for the improved coverage of this material have to be developed to provide better functionality and stability. Direct proportionality between the SAM 2D-DLP and the IR absorption intensity, observed as a function of molecular chain-length, suggest that the uniformly polarized medium of the SAM enhances the electronic component of the molecular polarizability. The corresponding IR absorption enhancement is reflected in a change to the SAM dielectric constants. Electrostatic surface phenomena such as this are expected to influence the PL intensity originating from the GaAs substrate. For example, *in situ* PL measurements demonstrate that it is possible to follow the real-time process of alkanethiol SAM formation on GaAs. Thus, it seems reasonable that some other functionalization steps related to the sulfurization of the GaAs surface and/or hybridization of functionalized SAMs with targeted bio-moieties could be monitored with this technique.

Acknowledgements

We greatly acknowledge the financial support provided for the research reported here by the Canadian Institutes of Health Research, the Natural Sciences and Engineering Research Council of Canada (Project STPGP 350501-07) and the Canada Research Chair in Quantum Semiconductors Program. Computational resources

were provided by the Réseau québécois de calcul de haute performance (RQCHP). We thank Drs. Farid Bensebaa and Gregory Lopinski of the National Research Council of Canada (NRCC) for fruitful collaboration. One of us (GMM) thanks NRCC for providing a Graduate Student Scholarship Supplement award.

References

- [1] R.R. Kale, H. Mukundan, D.N. Price, J.F. Harris, D.M. Lewallen, B.I. Swanson, J.G. Schmidt, S.S. Lyer, *J. Am. Chem. Soc.* 130 (2008) 8169.
- [2] X.D. Hoa, A.G. Kirk, M. Tabrizian, *Biosens. Bioelectron.* 23 (2007) 151.
- [3] L. Nicu, T. Leichle, *J. Appl. Phys.* 104 (2008) 111101.
- [4] Z. Zhao, I.A. Banerjee, H. Matsui, *J. Am. Chem. Soc.* 127 (2005) 8930.
- [5] K.L. Brogan, M.H. Schoenfish, *Langmuir* 21 (2005) 3054.
- [6] L.M.S. Dora Peelen, *Langmuir* 21 (2005) 266.
- [7] O.S. Nakagawa, S. Ashok, C.W. Sheen, J. Martensson, D.L. Allara, *Jpn. J. Appl. Phys. Part 1 (Regular Papers Short Notes & Review Papers)* 30 (1991) 3759.
- [8] G.N.F. Sharon, R. Lunt, P.G. Santangelo, N.S. Lewis, *J. Appl. Phys.* 70 (1991) 7449.
- [9] J.F. Dorsten, J.E. Maslar, P.W. Bohn, *Appl. Phys. Lett.* 66 (1995) 1755.
- [10] S.Y.T. Baum, K. Uosaki, *Langmuir* 15 (1999) 8577.
- [11] C.L. McGuinness, A. Shaporenko, C.K. Mars, S. Uppili, M. Zharnikov, D.L. Allara, *J. Am. Chem. Soc.* 128 (2006) 5231.
- [12] Y. Jun, X.Y. Zhu, J.W.P. Hsu, *Langmuir* 22 (2006) 3627.
- [13] F. Seker, K. Meeker, T.F. Kuech, A.B. Ellis, *Chem. Rev.* 100 (2000) 2505.
- [14] J.J. Dubowski, *Quantum Dot Bio-template for Rapid Detection of Pathogenic Substances*, in: NATO Science Series, vol. 239, Springer, Dordrecht, 2006, pp. 159–173.
- [15] J.J. Dubowski, *Lasers and Electro-Optics Society, LEOS 2006, 19th Annual Meeting of the IEEE* vol. 0-7803-9556-7, Montreal, 2006, pp. 302–303.
- [16] J.J. Dubowski, X. Ding, E.H. Frost, E. Escher, *US Patent* 2006/11/908,223.
- [17] M. Bruchez Jr., M. Moronne, P. Gin, S. Weiss, A.P. Alivisatos, *Science* 281 (1998) 2013.
- [18] S. Hohng, T. Ha, *J. Am. Chem. Soc.* 126 (2004) 1324.
- [19] C.K. Kim, G.M. Marshall, M. Martin, M. Bisson-Viens, Z. Wasilewski, J.J. Dubowski, *J. Appl. Phys.* 106 (2009) 083518.
- [20] S.R. Lunt, G.N. Ryba, P.G. Santangelo, N.S. Lewis, *J. Appl. Phys.* 70 (1991) 7449.
- [21] P.D.K.C.W. Wilmsen, J.M. Woodall, *J. Appl. Phys.* 64 (1998) 3287.
- [22] O. Voznyy, J.J. Dubowski, *J. Phys. Chem. B* 110 (2006) 23619.
- [23] O. Voznyy, J.J. Dubowski, *J. Phys. Chem. C* 112 (2008) 3726.
- [24] M.V. Lebedev, *Semiconductors* 42 (2008) 1048.
- [25] S. Tang, Z. Cao, *J. Phys. Chem. A* 113 (2009) 5685.
- [26] M. Saavedra, A. Buljan, M. Muñoz, *J. Mol. Struct. Theochem.* 906 (2009) 72.
- [27] C.L. McGuinness, A. Shaporenko, M. Zharnikov, A.V. Walker, D.L. Allara, *J. Phys. Chem. C* 111 (2007) 4226.
- [28] K. Adlkofer, M. Tanaka, *Langmuir* 17 (2001) 4267.
- [29] M.D. Pashley, *Phys. Rev. B* 40 (1989) 10481.
- [30] P.A. Redhead, *Vacuum* 12 (1962) 203.
- [31] N. Camillone III, K.A. Khan, R.M. Osgood Jr., *Surf. Sci.* 453 (2000) 83.
- [32] N.K. Singh, D.C. Doran, *Surf. Sci.* 422 (1999) 50.
- [33] S. Donev, N. Brack, N.J. Paris, P.J. Pigram, N.K. Singh, B.F. Usher, *Langmuir* 21 (2005) 1866.
- [34] T.P. Huang, T.H. Lin, T.F. Teng, Y.H. Lai, W.H. Hung, *Surf. Sci.* 603 (2009) 1244.
- [35] C.L. McGuinness, D. Blasini, J.P. Masejewski, S. Uppili, O.M. Cabarcos, D. Smilgies, D.L. Allara, *ACS Nano* 1 (2007) 30.
- [36] O. Voznyy, J.J. Dubowski, *Langmuir* 24 (2008) 13299.

- [37] W.G. Schmidt, F. Bechstedt, J. Bernholc, *Appl. Surf. Sci.* 190 (2002) 264.
- [38] O. Voznyy, J.J. Dubowski, *Langmuir* 25 (2009) 7353.
- [39] O. Voznyy, J.J. Dubowski, J.T. Yates, P. Maksymovych, *J. Am. Chem. Soc.* 131 (2009) 12989.
- [40] H. Ohno, L.A. Nagahara, W. Mizutani, J. Takagi, H. Tokumoto, *Jpn. J. Appl. Phys. Part 1 (Regular Papers Short Notes & Review Papers)* 38/1A (1999) 180.
- [41] K. Moumanis, X. Ding, J.J. Dubowski, E.H. Frost, *J. Appl. Phys.* 100 (2006) 034702.
- [42] R. Stine, D.Y. Petrovykh, *J. Electron Spectrosc. Rel. Phenom.* 172 (2009) 42.
- [43] S. Ye, G. Li, H. Noda, K. Uosaki, M. Osawa, *Surf. Sci.* 529 (2003) 163.
- [44] A. Shaporenko, K. Adlkofer, L.S.O. Johansson, M. Tanaka, M. Zharnikov, *Langmuir* 19 (2003) 4992.
- [45] Q. Zhang, H. Huang, H. He, H. Chen, H. Shao, Z. Liu, *Surf. Sci.* 440 (1999) 142.
- [46] C. van der Marel, M. Yidirim, H.R. Stapert, *J. Vac. Sci. Technol. A* 23 (2005) 1456.
- [47] R.W. Paynter, *Surf. Interface Anal.* 27 (1999) 103.
- [48] G. Neshet, A. Vilan, H. Cohen, D. Cahen, F. Amy, C. Chan, J.H. Hwang, A. Kahn, *J. Phys. Chem. B* 110 (2006) 14363.
- [49] D.M. Rosu, J.C. Jones, J.W.P. Hsu, K.L. Kavanagh, D. Tsankov, U. Schade, N. Esser, K. Hinrichs, *Langmuir* 25 (2009) 919.
- [50] G.M. Marshall, G.P. Lopinski, F. Bensebaa, J.J. Dubowski, *Langmuir* 25 (2009) 13561.
- [51] G.M. Marshall, F. Bensebaa, J.J. Dubowski, *J. Appl. Phys.* 105 (2009) 094310.
- [52] X.M. Ding, K. Moumanis, J.J. Dubowski, L. Tay, N.L. Rowell, *J. Appl. Phys.* 99 (2006) 054701.
- [53] D.M. Wieliczka, X.M. Ding, J.J. Dubowski, *J. Vac. Sci. Technol. A* 24 (2006) 1756.
- [54] H. Wang, S. Chen, L. Li, S. Jiang, *Langmuir* 21 (2005) 2633.
- [55] X. Ding, K. Moumanis, J.J. Dubowski, E.H. Frost, E. Escher, *Appl. Phys. A: Mater. Sci. Process.* 83 (3) (2006) 357–360.
- [56] V. Duplan, Y. Miron, E. Frost, M. Grandbois, J.J. Dubowski, *J. Biomed. Opt.* 14 (2009) 054042.
- [57] H. Hasegawa, M. Akazawa, *Appl. Surf. Sci.* 254 (2008) 8005.
- [58] Y.T. Wu, J.D. Liao, C.C. Weng, Y.T. Hsieh, C.H. Chen, M.C. Wang, M. Zharnikov, *J. Phys. Chem. C* 113 (2009) 4543.